Chemistry Research Journal, 2024, 9(3):190-201
Available online www.chemrj.org

Research Article

ISSN: 2455-8990
CODEN(USA): CRJHA5

Synthesis, molecular docking as anti-prostate cancer, and biological evaluation of ceftazidime transition metal complexes

Gehan S. Elasala[1], Alaa E. Ali[1], Wahed A. Gad[2], Sherif A. Kolkaila[1*]

[1]Department of chemistry, Faculty of science, Damanhour University, Egypt
[2]Institute of Graduate studies and Environmental Research, Damanhour University, Egypt
*Corresponding author's Email address: sherifak@Sci.dmu.edu.eg

Abstract The synthesis, characterization, and thermal analysis of ceftazidime complexes with transition metals (Cr(III), Mn(II), Co(II), Ni(II), Cu(II), Zn(II), Cd(II), and Hg(II) were discussed. Ceftazidime is found to serve as a bidentate ligand. From magnetic measurements and spectral data, octahedral structures were hypothesized for all complexes except (Co, Ni, and Hg), which possessed tetrahedral structures. Ceftazidime complexes exhibit more action than commercial ceftazidime against specific pathogens. Thermal breakdown processes for ceftazidime and its metal complexes were proposed based on TG and DTA curves. Except for the Hg complex, the thermal breakdown resulted in the creation of metal oxides and carbon residue as a final product.

Keywords Cephalosporins complexes– ceftazidime Complexes –Thermal analysis-biological activity

Introduction

Ceftazidime is the third generation of cephalosporins Fig. (1). Ceftazidime is regarded as one of the most significant medications required in the basic health system for the treatment of various infections, including joint infections and vibrio infections. Ceftazidime's structure includes a beta lactam ring and is resistant to β-lactamases produced by bacteria [1]. In this study, conformational alterations and biding of ceftazidime towards transition metals were discovered using IR, electronic spectra, and magnetic susceptibility. The thermal analysis of ceftazidime and its metal complexes was also explored using thermogravimetric and differential analysis curves. Additionally, the mechanism of decomposition is explained. The kinetic parameters were studied. Molecular docking of some complexes as anti- prostate cancer is done.

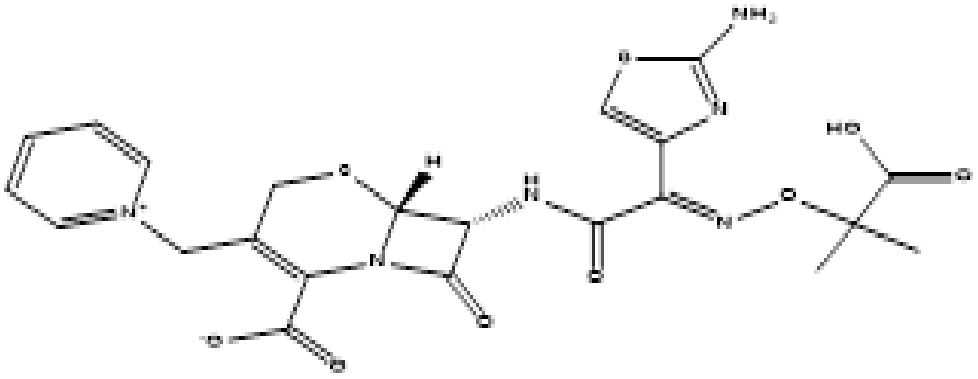

Figure 1: Structure of Ceftazidime, HL

Experimental

Ceftazidime solution was added to hot ethanol, Cr (III) aqueous solution was added at a molar ratio of 1:1. The mixture had been refluxed for 24 hours. The resulting solution was filtered and reduced to half of its original volume by solvent evaporation. The concentrated solution was kept overnight at room temperature, resulting in the creation of a solid product. It was filtered, rinsed with a tiny amount of ethanol, and dried. All additional complexes were made in the same way, using the relevant metal salts as chloride. Tables 1 and 2 contain physical measurements, analytical results, and spectrum data for the complexes.

Measurements

Ceftazidime and all complexes were analyzed for carbon, hydrogen, sulphur, and nitrogen at Cairo University's central lab using CHNS Nr.11042023. The chloride contents of the complexes were determined using the classic Volhard method [2]. The Perkin Elmer spectrophotometer, Model 1430, was used to record the infrared spectra of ceftazidime and its metal complexes. The solid complexes' electronic spectra were measured in Nujol mull spectra [3]. Molar magnetic susceptibilities, constants were determined using Faraday's method at room temperature 25°C. A Shimadzu DTA/TGA-60 was used to perform differential thermal analysis (DTA) and thermogravimetric analysis (TG) of ceftazidime and its complexes. The heating rate was 20 °C per minute. The atmospheric nitrogen flow rate was 15 milliliters per minute, and the cell utilized was platinum. Ceftazidime and its metal complexes were biologically screened against ten different microbial species. These included one Gram-positive (Staphlococcus aureas), four Gram-negative (Escherichia Coli ATCC 8739 strain, Streptococcus Faecalis, Pesudomonas Aeruginosa, and Vibrio damsela) bacteria, and five fungi (Fusarium solani, penicillium orayzae, penicillium oxide, Aspergillus flavus, and Aspergillus niger). Nine molecules, the ligand ceftazidime, and eight complexes of various metal ions were included in the investigation. Levofloxacin, Vancomycin, Imipenem, and Amikacin are the four distinct broad-spectrum antibiotics that are utilized as references in this work.

Table 1: Elemental analysis, m.p. and colour of ceftazidime complexes

Complexes	Colour	Calculated/(Found)%					
		C	**H**	**N**	**S**	**M**	**Cl**
$[Cr(L)_2Cl(H_2O)]$	Dark violet	39.63 (36.64)	3.90 (3.99)	14.07 (13.99)	9.20 (9.65)	7.46 (7.73)	5.09 (5.03)
$[Mn(HL_2)Cl(H_2O)]$	Yellow	39.46 (39.56)	3.89 (3.82)	14.01 (14.51)	9.16 (9.44)	7.85 (7.61)	5.06 (5.03)
$[Co(L)Cl H_2O]$	Orange	40.16 (40.71)	3.67 (3.92)	12.75 (12.66)	9.73 (9.82)	8.94 (8.13)	8.35 (8.99)
$[Ni(L)Cl(H_2O)]$	Green	40.11 (40.82)	3.67 (3.91)	12.76 (12.66)	9.74 (9.92)	8.91 (8.60)	5.38 (5.99)
$[Cu(HL_2)Cl(H_2O)]$	Brown	43.52 (43.66)	4.15 (4.11)	13.84 (13.77)	10.56 (10.50)	5.23 (5.19)	2.42 (2.38)
$[Zn(L)Cl(H_2O)]$	Yellow	30. 80 (30.62)	2.93 (2.78)	12.52 (12.34)	7.16 (7.62)	14.61 (14.23)	15.84 (15.98)
$[Cd_2(HL_3)(Cl)_2(H_2O)_2]$	Yellow	28.13 (28.40)	2.90 (2.62)	11.93 (11.82)	6.83 (6.92)	23.93 (23.91)	7.55 (7.27)
$[Hg(L)Cl(H_2O)]$	Dark yellow	33 (33.05)	3.02 (3.33)	10.50 (10.3)	8.01 (8.02)	25.05 (25.1)	4.43 (4.33)

All the complexes have m.p > 300º C

Results and Discussion

From IR spectra of ceftazidime and their metal complexes Table (3), it's obtained that ceftazidime complexes show broad bands in the 3318 – 3419 cm^{-1} regions in all prepared complexes suggesting coordination with water. It seems from the elemental analysis of the complexes and thermal analysis that all complexes contain water molecules in their structures, as evident by ν_{OH}, Table (7). The band of N-H stretching vibration of the hydrogen bonded NH_2 group appears at 3428 cm^{-1} in spectra of ceftazidime. This band appears in all simple complexes but overlapped with ν_{O-H} of H_2O broad bands. The ring carbonyl absorption frequency will be shifted to higher wave numbers as the ring becomes more and more strained. The lactam (C=O) band appears at 1758 cm^{-1} in the spectrum of ceftazidime which is shifted in the simple complexes spectra (1758 -1782 cm^{-1}) range. The amide C=O-NH band appears at 1687 cm^{-1} in the spectrum of ceftazidime while the complexes show this band at 1661- 1687 cm^{-1}, suggesting that ligand coordination with these metal ions occurs through the oxygen from the lactam carbonyl group rather than the amide carbonyl group, where the shifting was not significant in the far IR spectra, the bonding of oxygen is provided by the presence of bands at 437.5 cm^{-1} (M-O) [4-8].

Table 2: Fundamental infrared bands (cm^{-1}) of ceftazidime and its metal complexes

Compound	ν_{NH}	ν(C=O) lactam	ν(C=O) amide	ν (COO) asym	ν (COO) sym	ν (C-N) of β-lactam	ν_{C-O} stretch	ν_{M-N}	ν_{M-O}	ν_{M-Cl}
Ceftazidime	3425	1770	1677	1610	1364	1461	1011	-	-	-
[Cr $(L)_2Cl(H_2O)$]	3290	1776	1674	1615	1364	1460	1012	435	401	342
[Mn $(HL_2)Cl(H_2O)$]	3298	1767	1675	1615	1365	1461	1013	495	407	342
[$Fe_2(L)_3Cl_2(H_2O)(OH)$]	3295	1782	1675	1615	1365	1461	1015	476	406	342
[Co(L) Cl H_2O]	3392	1776	1676	1615	1365	1462	1011	487	403	360
[Ni (L) $Cl(H_2O)$]	3293	1776	1675	1615	1393	1462	1012	480	402	362
[Cu $(HL_2)Cl(H_2O)$]	3428	1758	1657	1614	1375	1461	1018	470	405	362
[Zn(L)$Cl(H_2O)$]	3296	1776	1675	1615	1387	1461	1017	467	411	392
[Cd_2 (HL_3) $(Cl)_2(H_2O)_2$]	3297	1776	1675	1615	1368	1462	1019	470	424	377
[Hg(L) $Cl(H_2O)$]	3284	1770	1673	1614	1364	1459	1012	470	425	342

Electronic spectral and magnetic studies

The electronic absorption spectra and effective magnetic moment values, give us the information to suggest structure geometry as listed in **Table (3)**, However, Zn,Hg and Cd complexes exhibited only a high intensity band at 200-255 nm, which are assigned to ligand →metal charge transfer. Owing to the d10- configuration of Zn(II), Cd(II) and Hg(II), no d-d transition could be observed and therefore the strerochemistry around these metals in its complexes can be hardly determined [9].

Table 3: Nujol mull electronic absorption spectra λ_{max} (nm), room temperature effective magnetic moment values (μ_{eff}, 298°K) and geometries of ceftazidime metal complexes

Complex	λ_{max} (nm)	Transitions	μ_{eff}	Geomety
$[Cr(L)_2Cl(H_2O)]$	208, 427, 461	$^4A_{2g}\rightarrow{}^4T_{2g}(F)$, $^4A_{2g}\rightarrow{}^4T_{1g}(F)$ $^4A_{2g}\rightarrow{}^4T_{1g}(p)$	4.8	O_h
$[Mn(HL_2)Cl(H_2O)]$	446,638	$^6A_{1g}\rightarrow{}^4T_{1g}$ $^6A_{1g}\rightarrow{}^4T_{2g}$ $^6A_{1g}\rightarrow{}^4T_{1g}$	5.8	O_h
$[Co(L)\,Cl\,H_2O]$	340, 432, 516	$^4A_2\rightarrow{}^4T_1(P)$	4.3	T_d
$[Ni(L)\,Cl(H_2O)]$	427, 634	$^3T_1(F)\rightarrow{}^3T_1(P)$ $^3T_{1(F)}\rightarrow{}^3A_2$	3.1	T_d
$[Cu(HL_2)Cl(H_2O)]$	212, 435	$^2T_2\rightarrow{}^2E_g$	1.73	O_h
$[Zn(L)Cl(H_2O)]$	234	------	Diamagnetic	O_h
$[Cd_2(HL_3)(Cl)_2(H_2O)_2]$	265	------	Diamagnetic	O_h
$[Hg(L)\,Cl(H_2O)]$	229	-------	Diamagnetic	T_d

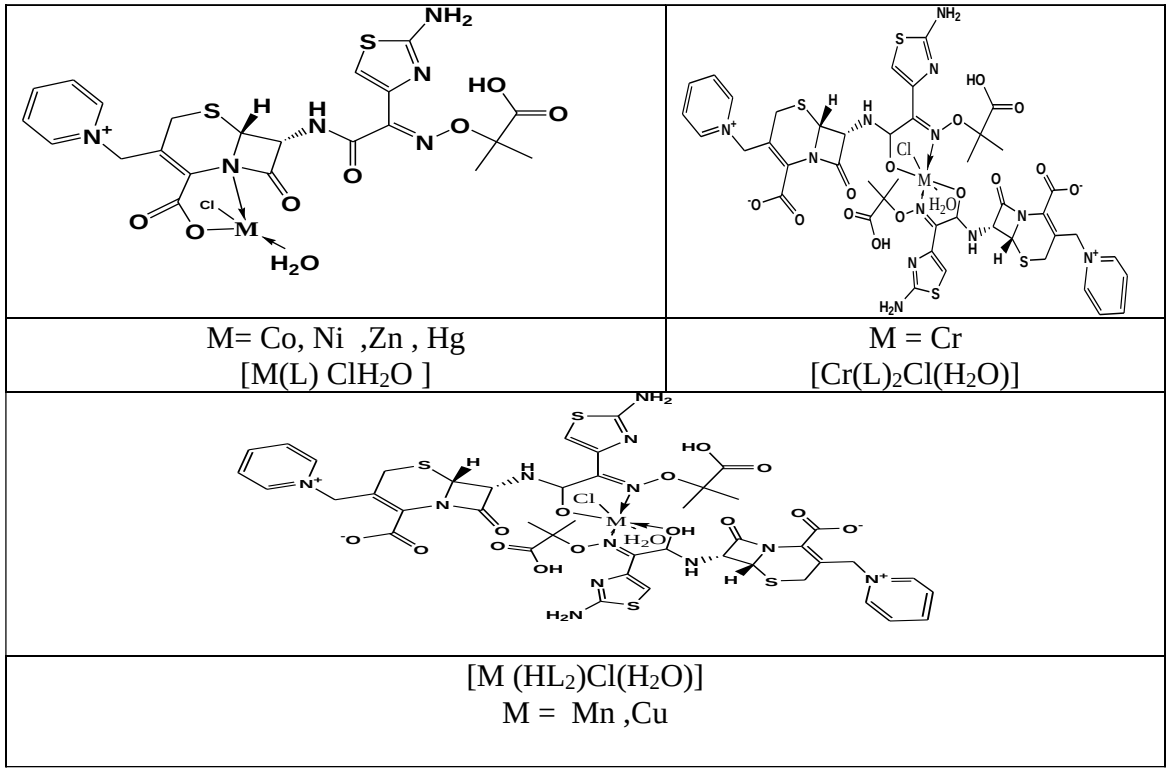

Figure 2: Proposed structures of ceftazidime complexes

Biological activity

In this study, 10 microorganisms representing different microbial categories, {one Gram-positive (Staphylococcus *Aureas*), four Gram negative (*Escherichia Coli* ATCC 8739 strain, *Streptococcus Faecalis, Pesudomonas Aeruginosa and Vibrio Damsela*) bacteria and five fungi (*Fusarium Solani, penicillium orayzae, penicillium. Oxalicum, Aspergillus flavus and Aspergillus niger*)} were used. The study included 10 compounds, ligand (ceftazidime) and 9 complexes of different metal ions}. Four different broadly antibiotics (*Levofloxacin, Vancomycin, Imipenem and Amikacin*) are used in this study as references.

The data depicted in **Tables (4-7)** allow the following observations and conclusions:

All the investigated compounds have higher antibacterial activity compaired to antifungal activity. ligand (ceftazidime) showed similar activities for *S. aureus, P. aureginosa and E. coli*

[Cr (Ceftazidime)$_2$Cl(H$_2$O)] complex showed negative activity to *S. aureus, E. coli and V. damsela* while it showed a highly positive activity to *P. aureginosa*. It revealed by the diameter of its inhibition zone. It showed activity in the same range of ceftazidime for *S. faecalis.* On the other hand, [Mn (Ceftazidime)$_2$Cl(H$_2$O)] complex showed no antibacterial activity against all the bacteria screened except for *P. aureginosa*, it showed activity in the same range of cefotaxime.

The highest antibacterial activity were shown by the [Co(ceftazidime)Cl H$_2$O] and [Ni (Ceftazidime)Cl(H$_2$O)] complexes against *P. aureginosa and S. faecalis* compared to ceftazidime and the reference antibiotics while [Zn$_2$(Ceftazidime)$_3$(Cl)$_4$] complex showed a lower antimicrobial activity than ceftazidime against all bacteria screened. The [Cu (Ceftazidime)$_2$Cl(H$_2$O)] complex showed activity in the range of ceftazidime against all bacteria screened.

On the other hand, [Cd$_2$ (ceftazidime)$_3$(Cl)$_2$(H$_2$O)$_2$] complex showed a high positive activity to *S. aureus, E. coli and P. aureginosa* while it showed activities close to ceftazidime for the rest bacteria screened. For *V. damsela*, [Hg(ceftazidime)Cl(H$_2$O)] complex showed the highest antibacterial activity.

Compared to free ligands, the majority of metal complexes exhibit greater activity [10]. Based on chelation theory and overtone idea, the higher activity of the metal chelates might be explained [11]. Permeability of the cell the lipid barrier enveloping the cell facilitates the passage of solely lipid soluble substances, as liposolubility plays a crucial role in regulating antimicrobial efficacy. Due to the ligand orbital overlap and partial sharing of the metal ion's positive charge with the donor groups during chelation, the polarity of the metal ion is lowered to a higher extent. Additionally, it improves the complex's lipophilicity and boosts the delocalization of p- and d-electrons throughout the whole chelate. The complexes' enhanced ability to penetrate lipid membranes and obstruct metal binding sites on the microorganism's enzymes is facilitated by their increased lipophilicity.

From MIC measurements **Table (5)**, our conclusion that *P. aureginosa* is more sensitive to [Co(ceftazidime)Cl H$_2$O] and [Ni (Ceftazidime)Cl(H$_2$O)]complexes and these confirmed positive activity for these two complexes.

Table 4: Antibacterial activity of the investigated compounds against some reference trains expressed in absolute activity (AU)

Compound	Antibacterial activity (AU)				
	S. aureus	***E. coli***	***S. feacalis***	***P. aureginosa***	***V. damsela***
ceftazidime	10	13.4	13.4	25	9
[Cr (Ceftazidime)$_2$Cl(H$_2$O)]	-	-	16	44.4	-
[Mn (Ceftazidime)$_2$Cl(H$_2$O)]	-	-	-	18.8	4
[Fe$_2$(Ceftazidime)$_3$Cl(H$_2$O)$_2$]	-	12.3	10	27.8	-
[Co(ceftazidime)Cl H$_2$O]	23.7	-	23.7	62.7	9.3
[Ni (Ceftazidime)Cl(H$_2$O)]	10	-	22.5	80.3	7
[Cu (Ceftazidime)$_2$Cl(H$_2$O)]	9	11.1	16	18.8	13.4
[Cd$_2$ (ceftazidime)$_3$(Cl)$_2$(H$_2$O)$_2$]	20.9	27.8	14.9	31.6	12.3
[Hg(ceftazidime)Cl(H$_2$O)]	12.3	10	20.9	27.8	31.6

Table 5: The minimal inhibitory concentrations (MICs) (mg/ml) of the investigated compounds expressed as AU

Compound	MIC				
	S. aureus	***E. coli***	***S. feacalis***	***P. aureginosa***	***V. damsela***
ceftazidime	90	-	-	40	80
[Cr (Ceftazidime)$_2$Cl(H_2O)]	-	-	50	10	-
[Mn (Ceftazidime)$_2$Cl(H_2O)]	-	-	-	50	100
[Co(ceftazidime)Cl H_2O]	50	-	50	5	70
[Ni (Ceftazidime)Cl(H_2O)]	80	-	30	2	80
[Cu (Ceftazidime)$_2$Cl(H_2O)]	80	70	70	60	70
[Zn_2(Ceftazidime)$_3$($Cl)_4$]	100	-	-	90	100
[Cd_2 (ceftazidime)$_3$($Cl)_2$($H_2O)_2$]	50	40	70	40	80
[Hg(ceftazidime)Cl(H_2O)]	80	60	60	50	50

Table 6: Commercial antibiotics effect on the same reference bacterial strains

Antibiotic	Reference strains				
	S. aureus	***E. coli***	***S. feacalis***	***P. aureginosa***	***V. damsela***
Levofloxacin	-	-	24	-	-
Vancomycin	25	24	-	-	-
Imipenem	45	38	37	-	35
Amikacin	-	-	15	-	-

Table 7: The antifungal activity of the free ligands and its complexes against some reference strains expressed in absolute activity (AU)

Compound	Antifungal activity (AU)				
	A. flavus	***A. niger***	***F. solani***	***P. orayzae***	***P. oxalicum***
ceftazidime	-	-	-	-	-
[Cr (Ceftazidime)$_2$Cl(H_2O)]	-	-	-	-	-
[Mn (Ceftazidime)$_2$Cl(H_2O)]	-	-	-	-	-
[Co(ceftazidime)Cl H_2O]	-	-	40	-	-
[Ni (Ceftazidime)Cl(H_2O)]	-	54	28	-	-
[Cu (Ceftazidime)$_2$Cl(H_2O)]	-	-	28	-	-
[Zn_2(Ceftazidime)$_3$($Cl)_4$]	-	-	28	-	-
[Cd_2 (ceftazidime)$_3$($Cl)_2$($H_2O)_2$]	-	-	40	-	54
[Hg(ceftazidime)Cl(H_2O)]	-	-	28	-	-

Thermal Analysis

Masoud et al. have reported on the temperature behavior of a few physiologically active chemicals [12–19]. Thermograms (TG and DTA) were used to examine the thermal behavior of ceftazidime and metals (II) complex, as illustrated in Figure (5). Ceftazidime undergoes exothermic breakdown, with the exception of the first step, which is endothermic. Up to 80 °C, there is no mass loss. The DTA curve has an endothermic effect as the first stage of decomposition, which has a weight loss of 3.11% and commences at 25°C and finishes at 80°C. The breakdown reaches its second stage between 81 and 200 °C (20.96% weight loss). Concurrently, the DTA curve confirms weight loss and displays an exothermic effect in the 160 °C range. The DTA curve has an exothermic impact as the third stage of decomposition, which has a weight loss of 44.92% and commences at 201°C and concludes at 280°C. At 281 °C, the final stage of disintegration begins, and it ends at 600 °C (82.43% weight loss). In the meantime, weight loss confirms the exothermic effect seen in the DTA curve in the 470 °C region.

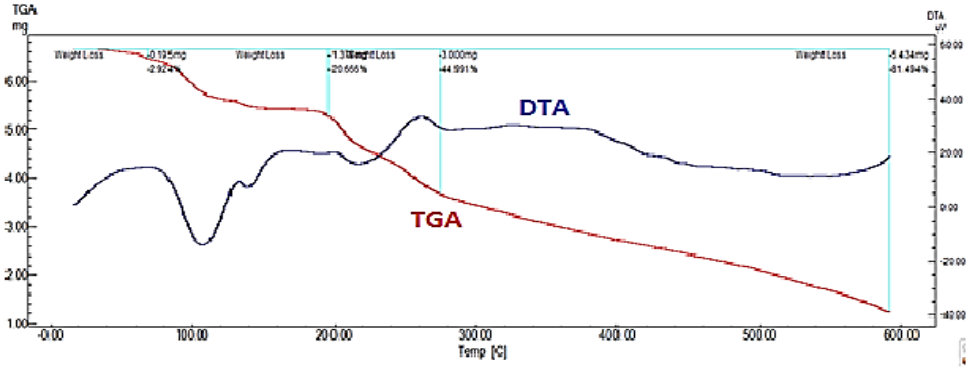

Figure 3: TGA and DTA of ceftazidme ligand

The suggested mechanism is given as follows:

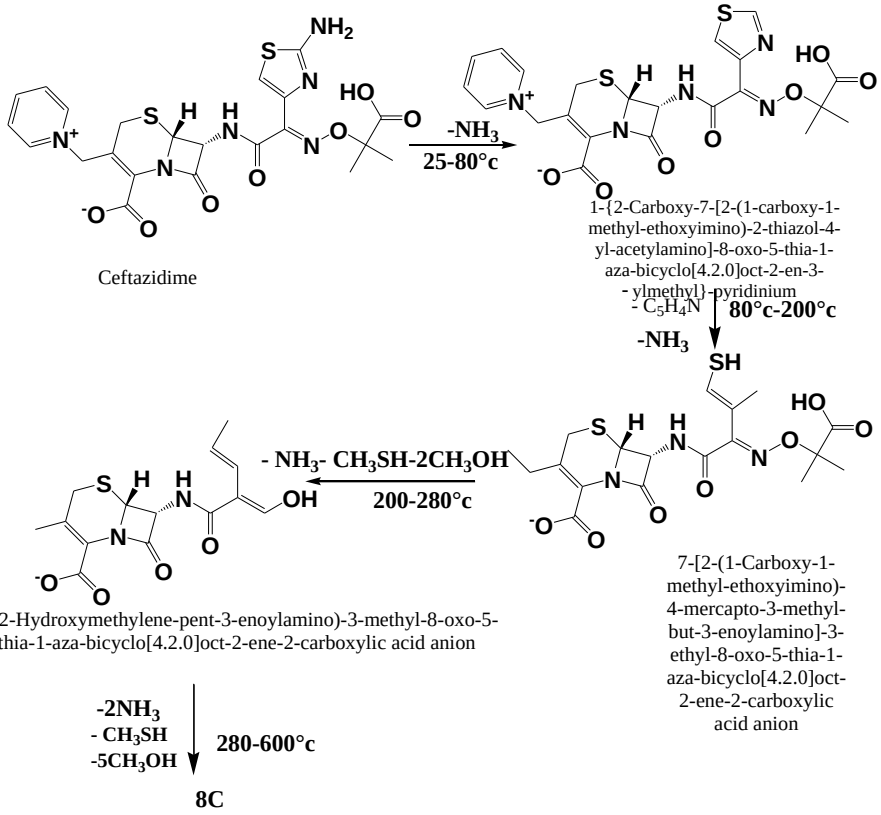

Scheme (1):Thermolysis of ceftazidime legand

As an example for [Cr $(L)_2Cl(H_2O)$] complex Figure: (4) the DTA curve exhibits an endothermic effect in the range of 137.2 °C, which is followed by weight loss indicating the first stage of decomposition, which begins at 27 °C and ends at 174 °C with a corresponding weight loss of 17.51%. The breakdown phases II were detected between 175 and 453 °C (58.87 % weight loss). Exothermic impact is visible in the DTA curve at the 260 °C range. At 445 °C, the final stage of disintegration begins, and it terminates at 580 °C (89. 92% weight loss). The DTA curve shows an exothermic effect in the 488.5 °C range, which is supported by weight loss.

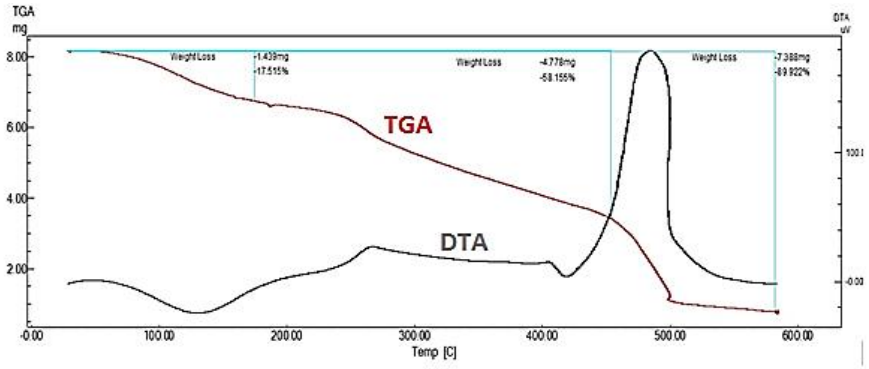

Figure (4): TGA and DTA of Cr- ceftazidme complex

The suggested mechanism is given as follows:

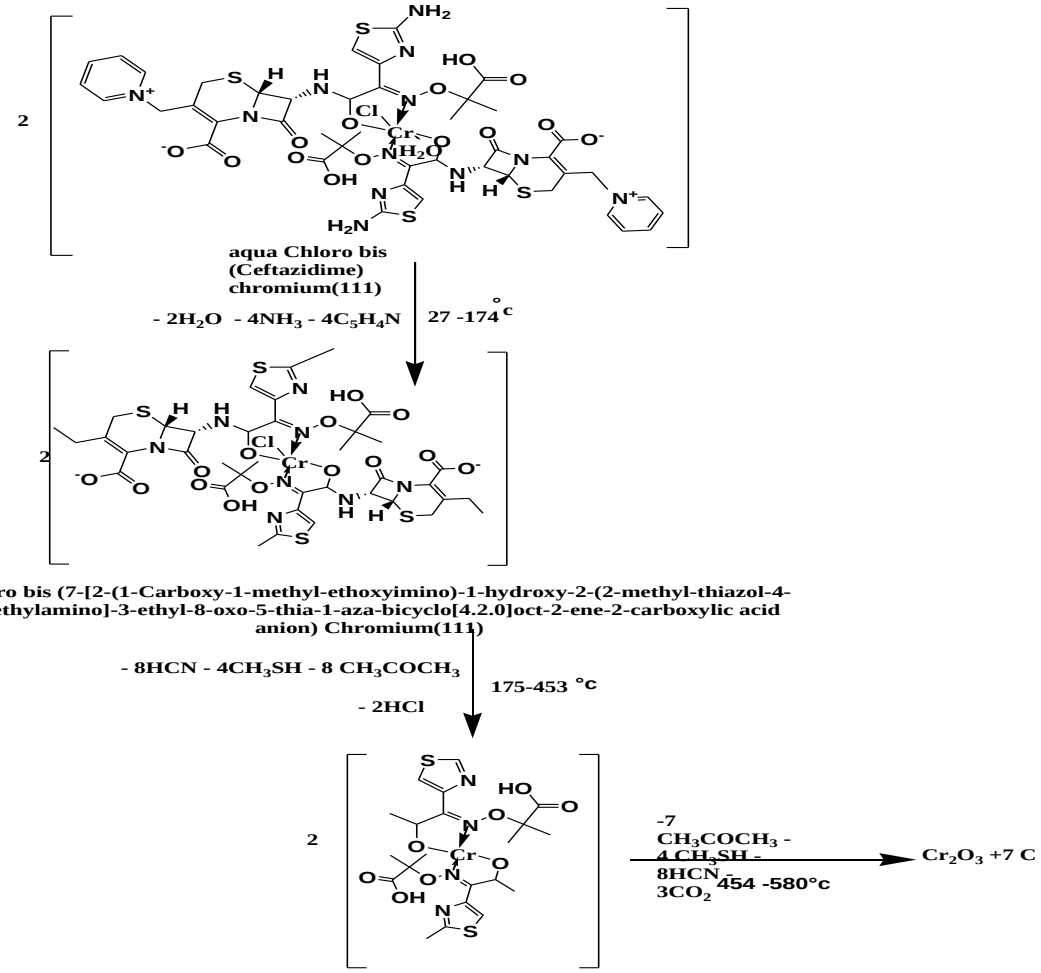

Scheme (2): themolysis of [Cr (L)$_2$Cl(H$_2$O)]

Zn-ceftazidime complex

The docked ligand (Zn-ceftazidime complex) with 6XXO protein which is responsible for prostate cancer Fig. (5 In most cases, the electrostatic and hydrogen bond lengths between the ligand and receptor were ≤ 3.3 A, indicating the presence of typical real bonds and strong binding affinity (Fig. 5). For example, the closest interaction is observed via H-donors with 6XX0 (2.7A) and Zn-ceftazidime complex). With Moldock score (S) 63506 kcal, 8 binding sites of the designed drug with different amino acids (Arg 88,Glu 89,Pro 41, and Thr 91) were observed, demonstrating their ability to inhibit prostate cancer [20-23].

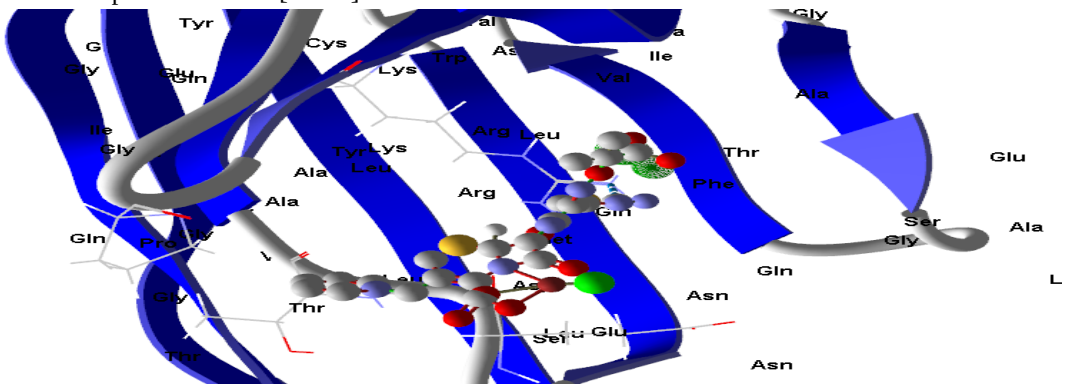

Figure 5: Virtual Molecular docking of the best docked (Zn-ceftazidime complex) with 6XXO protein

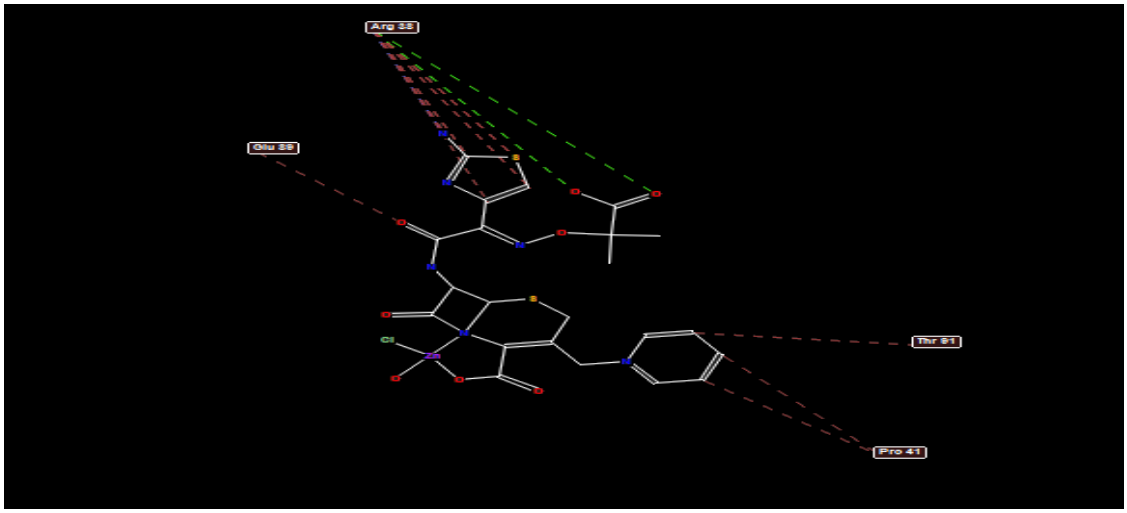

Figure 6: 2D structure of Molecular docking of (Zn-ceftazidime-complex) with 6XX0 protein

While the developed drugs (cobalt ceftazidime complex) is docked with the 6XXO prostate cancer protein, Fig. (7) indicates a stronger electrostatic and hydrogen interaction between the complex and receptor than the ligand. The nearest contact is detected via H-donors with 6XX0 (2.90A) and (cobalt ceftazidime complex), which suggests the presence of typical real bonds, implying high binding affinity. With a Moldock score of 63541 kcal, eight binding sites of the intended medication with distinct amino acids (Arg 38, Glu 89, and Pro 41) were identified, confirming their stronger inhibition than the ligand.

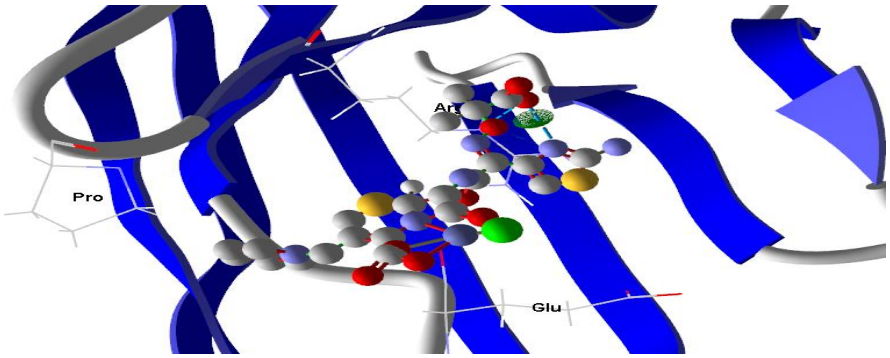

Figure 7: Virtual Molecular docking of the best docked (Co-ceftazidime-complex) with 6XX0 protein

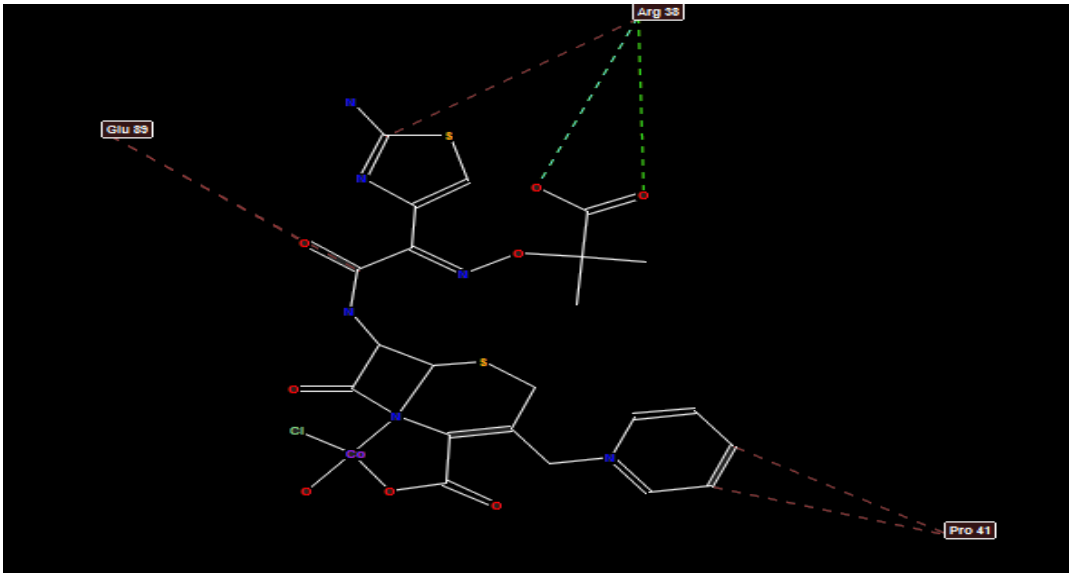

Figure (8):2D structure of Molecular docking of (Co-ceftazidime-complex) with 6XX0 protein

Cu –ceftazidime complex

The complex shows no inhibition for prostate cancer protein no torsions is obtained.

From the above data the best designed drugs complex's is Co-ceftazidime complex a promoting drug for inhibition of cancer prostate.

Conclusion

The synthesis, characterization, and thermal analysis of ceftazidime complexes with transition metals (Cr(III), Mn(II), Co(II), Ni(II), Cu(II), Zn(II), Cd(II), and Hg(II) were discussed. Ceftazidime is found to serve as a bidentate ligand. From magnetic measurements and spectral data, octahedral structures were hypothesized for all complexes except (Co, Ni, and Hg), which possessed tetrahedral structures. Ceftazidime complexes exhibit more action than commercial ceftazidime against specific pathogens. Thermal breakdown processes for ceftazidime and its metal complexes were proposed based on TG and DTA curves. Except for the Hg complex, the thermal breakdown resulted in the creation of metal oxides and carbon residue as a final product.

References

[1]. Joseph S., John E., John S., Keith A., Ellie J. C., Ellen J.,Patrick J., Anthony W., Soumitra R. , Sherwood Gorbach and John G. , Complicated Intra-abdominal Infection Guidelines,50(2010)133-164

[2]. Lee R.H, Griswold E. and Kleinberg J., Inorg. Chem. 3 (1964)1278-1283

[3]. Vogel A.I, A Text Book of Quantitative Inorganic Analysis, Longmans, London, (1989) 722-726.

[4]. Kolkaila S.A., Ali A.E. and Elasala G.S., Synthesis, Spectral Characterization of Azithromycin with Transition Metals and a Molecular Approach for Azithromycin with Zinc for COVID-19. Int J Cur Res Rev. (2021)13, 23, 53-59.

[5]. Masoud M.S., Ali A.E., Elasala G.S. and kolkaila S.A., Synthesis, spectroscopic, biological activity and thermal characterization of ceftazidime with transition metals. Spectrochim. Acta. (2018) 193, 458-466.

[6]. Ali A. E., Elasala G. S., Mohamed E. A. and kolkaila S.A., Spectral, thermal studies and biological activity of pyrazinamide complexes heliyon, (2019) 5(11)

[7]. Ali A.E., Elasala G.S., Mohamed E. A. and kolkaila S.A.,Structural and thermal analysis of some imipramine complexes. J. materials today proceeding.

[8]. Lee R.H, Griswold E, Kleinberg J. (1964), Inorg. Chem., (2021), 3, 1278-1283,. DOI= http://doi.org/10.1021/ic50019a018

[9]. Masoud M.S., Ali A.E., Elasala G.S. and kolkaila S.A., Synthesis, Spectroscopic Studies and Thermal Analysis on Cefoperazone Metal Complexes. J. Chem. Pharm. Res. (2017)9(4), 171-179.

[10]. Masoud M.S., Ali A.E., Elasala S. G., S.F sakr, kolkaila S.A.,Structural, Physicochemical Studies of Some Biologically Active Metal Complexes of Cefazolin Antibiotics J. Chem. Pharm. Res. (2020) 12, 42-52.

[11]. Timurs M. et al, Discovery of Protein-Protein Interaction Inhibitors by Integrating Protein Engineering and Chemical Screening Platforms. Cell Chemical Biology (2020) 27, 1441–1451

[12]. Kolkaila S.A., Ali A.E.,Doha Beltagy and Elasala G.S., Spectral and Biological Studies of Some Selected Thiouracil, Barbital and Thiobarbituric Acid Complexes. J Drug Des.Res. (2018) 5, 2, 1071-1079.

[13]. Howlader M. B. H, M. S. Islam and Karim M. R Synthesis of some 16-membered macrocyclic complexes of chrornium(III), manganese(II), iron(III), cobalt(II), nickel(II) and copper(II) containing a tetraoxooctaazacyclohexadecane ligand, J. Chem, (2000) 39 A, 407.

[14]. Ali A. E.Elmelegy E. , Kolkaila S. A., Mustafa A. A., Eledkawy A. M. and Alnaggar G. A. Removal of Cadmium (II) from Water by Adsorption on Natural Compound. Journal of Environmental Treatment Techniques, (2022) 10(2) 164-169.

[15]. Kolkaila S.A., Ali A.E., Mustafa Ahmed A. Removal of Aluminum (III) from Water by Adsorption on the Surface of Natural Compound. J. of Environmental Treatment Techniques2023. (2023) 11(2) 10-105.

[16]. Ali A.E., Elasala G.S., Rana M.Atta. and kolkaila S.A., Synthesis, Thermal Analysis and Characterization of Doxycycline Metal Complexeschemistry research journal. (2022) 7,2,90-91

[17]. Thorburn Burns D., Vogel's textbook of quantitative inorganic analysis, including elementary instrumental analysis 4th edn: revised by J. Bassett, R.C. Denney, G.H. Jeffery and J. Mendham, Longman, London and New York, (1978) 106, 925

[18]. Stuart MC, Kouimtzi M, Hill SR. WHO Model Formulary. World Health Organization., (2008) 137-139

[19]. Ali A. E., Elasala G. S., Eldeeb M. H., kolkaila S. A. Synthesis and Biological Activity and Thermal Analysis of Sulfaquinoxaline Mixed Metal Complexes. Journal of Chemistry & its Applications. (2022) SRC/JCIA-119.DOI: doi.org/10.47363/JCIA/2023(2)119

[20]. El-Tabl, A. S., El-Wahed, M. M. A. ., El Kadi, N. M., Kolkaila, S. A., & Samy, M.. Novel Metal Complexes of Bioactive Amide Ligands as New Potential Antibreast Cancer Agents. TWIST, (2023)18(4), 151-169.

[21]. El-Tabl, A. S., Kolkaila, S. A., Abdullah, S. M., & Ashour, A. M.. Nano-Organometallic Compounds as Prospective Metal BasedAnti-Lung Cancer Drugs: Biochemical and Molecular Docking Studies. TWIST, (2023) 18(4), 141-150.

[22]. El-Tabl, A. S., Dawood, A. A. E. R.., Kolkaila, S.A., Mohamed, E. H., & Ashour, A.. The Cytotoxicity of Some Biologically Active Nano Compounds against Colon Cancer: Advanced Biochemical Analyses. TWIST, (2023) 18(4), 360-371.

[23]. El-Tabl, A. S., Abd El-Wahed, M. M., Kolkaila, S. A., Abd El-Nasser, A. G., & Ashour, A. M.. Biochemical Studies on Some Novel Organometallic Complexes as Anti-Human Prostate Cancer. TWIST, (2024) 19(1),16-26